

PC-Sampler: Position-Aware Calibration of Decoding Bias in Masked Diffusion Models

Pengcheng Huang^{1*}, Shuhao Liu^{1*}, Zhenghao Liu¹, Yukun Yan²,
 Shuo Wang², Zulong Chen³, Tong Xiao¹

¹Department of Computer Science and Technology, Northeastern University, Shenyang, China

²Department of Computer Science and Technology, Institute for AI, Tsinghua University, Beijing, China

³Alibaba Group, Hangzhou, China

Abstract

Recent advances in masked diffusion models (MDMs) have established them as powerful non-autoregressive alternatives for sequence generation. Nevertheless, our preliminary experiments reveal that the generation quality of MDMs is still highly sensitive to the choice of decoding strategy. In particular, widely adopted uncertainty-based samplers suffer from two key limitations: a lack of global trajectory control and a pronounced bias toward trivial tokens in the early stages of decoding. These shortcomings restrict the full potential of MDMs. In this work, we introduce **Position-Aware Confidence-Calibrated Sampling** (PC-Sampler), a novel decoding strategy that unifies global trajectory planning with content-aware informativeness maximization. PC-Sampler incorporates a position-aware weighting mechanism to regulate the decoding path and a calibrated confidence score to suppress the premature selection of trivial tokens. Extensive experiments on three advanced MDMs across seven challenging benchmarks—including logical reasoning and planning tasks—demonstrate that PC-Sampler consistently outperforms existing MDM decoding strategies by more than 10% on average, significantly narrowing the performance gap with state-of-the-art autoregressive models. All codes are available at <https://github.com/NEUIR/PC-Sampler>.

1 Introduction

Large language models (LLMs) have recently achieved remarkable progress and profoundly shaped the development of artificial intelligence (DeepSeek-AI et al. 2025; Bai et al. 2023). Nearly all leading models follow the autoregressive (AR) paradigm, which has proven highly effective for complex reasoning tasks—particularly when combined with chain-of-thought (CoT) prompting (Wei et al. 2022). However, the rigid left-to-right generation order of AR models can be inefficient and restrictive for tasks that require more global or non-sequential reasoning, such as Countdown and Sudoku (Chen et al. 2023; Qin et al. 2025).

Masked Diffusion Models (MDMs) have emerged as a promising alternative, alleviating the sequential constraint of AR models by enabling flexible and non-autoregressive sequence generation through iterative denoising of masked tokens (Wu et al. 2025; Lou, Meng, and Ermon 2024). This flexibility broadens the generative modeling space and can

better capture dependencies in non-causal tasks (Ye et al. 2025a). Nevertheless, such increased flexibility introduces a new challenge: the sampling order itself becomes a crucial factor for model performance (Campbell et al. 2024). Consequently, there is increasing interest in principled sampling strategies (Christopher et al. 2025; Peng et al. 2025; Liu et al. 2025), with uncertainty-based sampling, which selects tokens based on model-internal uncertainty, emerging as the predominant approach due to its simplicity and effectiveness (Gong et al. 2025; Wang et al. 2025b).

Despite their promise, our preliminary experiments show that current uncertainty-based sampling strategies in advanced MDMs—such as LLaDA (Nie et al. 2025b), LLaDA-1.5 (Zhu et al. 2025), and Dream (Ye et al. 2025b)—face two critical challenges. First, they lack global trajectory control: by relying solely on locally greedy criteria, these methods cannot adapt the decoding order to task-specific structural demands, thereby limiting their applicability and the overall potential of MDMs. Second, they exhibit a strong trivial token bias, frequently selecting semantically uninformative tokens—such as punctuation and filler words—which results in wasted generation steps on low-information content and reduces the production of semantically meaningful outputs. To address these challenges, we propose PC-Sampler, a novel decoding strategy that unifies global trajectory control with content-aware informativeness maximization. PC-Sampler introduces a position-aware prior to flexibly guide the decoding trajectory and incorporates a frequency-calibrated confidence score to suppress the over-selection of trivial tokens, leading to more coherent and informative generation.

Our experiments on seven diverse and challenging benchmarks using three advanced MDMs demonstrate that our method consistently outperforms existing MDM decoding strategies, achieving average improvements of over 10%. Furthermore, PC-Sampler substantially narrows the performance gap with state-of-the-art autoregressive LLMs and, when applied to LLaDA-1.5, even surpasses comparably sized models such as Qwen-2.5-7B-Instruct. Additional analysis shows that PC-Sampler can be effectively combined with efficient sampling techniques, enabling significant acceleration of the decoding process while simultaneously improving generation quality. Collectively, these results highlight both the effectiveness and generalizability

*These authors contributed equally.

of our approach, which enhances generation quality in advanced MDMs without requiring any additional training.

2 Related Work

Building on the success of diffusion models in continuous domains such as image (Ho, Jain, and Abbeel 2020; Dhariwal and Nichol 2021) and audio synthesis (Kong et al. 2021), recent advances have successfully extended this paradigm to discrete text generation (Chang et al. 2022; Gong et al. 2023; Lou, Meng, and Ermon 2024). A key milestone in this direction is the Discrete Denoising Diffusion Probabilistic Model (D3PM) (Austin et al. 2021a), which formulates the diffusion process over discrete spaces as a fixed Markov chain with a learnable reverse transition. Among its specializations, Masked Diffusion Models (MDMs), also known as absorbing state diffusion, have emerged as a particularly promising direction due to their strong empirical performance (Nie et al. 2025a). The core idea of MDMs is to define a forward corruption process that progressively replaces text tokens with a special [MASK] token. This approach was first introduced in models such as DiffusionBERT (He et al. 2023) and has since been further improved by subsequent studies. Recent large-scale implementations—such as LLaDA (Nie et al. 2025b) and Dream (Ye et al. 2025b)—have shown that MDMs can scale up to 7–8 billion parameters and achieve performance comparable to autoregressive models of similar size. These advances establish MDMs as a compelling non-autoregressive alternative to traditional LLMs.

As large-scale MDMs continue to improve, their performance is becoming increasingly dependent on the choice of decoding strategy—especially the sampling algorithm—which governs the efficiency and quality of token generation (Kim et al. 2025). Current research in this area can be broadly grouped into three main directions. The first, and most central to generation quality, focuses on performant sampling—developing sophisticated token unmasking orders and methods to improve final output quality (Wang et al. 2025a; Peng et al. 2025; Liu et al. 2025). The second direction aims to improve efficiency by accelerating the inherently parallel yet iterative generation process, often through adaptive or fixed schedules that unmask multiple tokens per step (Park et al. 2025). The third line of work explores integrating MDMs with speculative decoding, using them as efficient “draft models” to accelerate larger autoregressive models (Chen et al. 2023; Christopher et al. 2025), thereby treating MDM efficiency as a complementary technology. Our work primarily falls within the first category, advancing the state of the art in generation quality.

At the heart of performant sampling lies the challenge of determining the optimal unmasking order (Wang et al. 2025a). Unlike autoregressive models that follow a fixed left-to-right order, MDMs can unmask tokens in any sequence. Each decoding order can be viewed as solving a different subproblem, and the difficulty of these subproblems can vary significantly (Kim et al. 2025), making the choice of an effective unmasking order crucial for generation quality (Peng et al. 2025). Overall, existing approaches to decoding order can be broadly categorized into three

classes. Heuristic-based methods rely on simple rules or predefined patterns, such as random selection. Uncertainty-based sampling typically adopts a greedy strategy that, at each step, selects the masked position with the highest confidence (e.g., lowest entropy (Koh et al. 2024; Ben-Hamu et al. 2025), highest maximum probability, or largest top- k confidence gap) for the next token reveal (Kim et al. 2025). Learning-based approaches explicitly optimize the unmasking trajectory, for example, by training a separate planner (Huang et al. 2025b). In addition, there are hybrid approaches that combine the strengths of autoregressive models and MDMs, offering a certain degree of global decoding order control. For example, semi-autoregressive schemes divide the sequence into blocks, decoding across blocks in a fixed order while using uncertainty-based decoding within each block (Arriola et al. 2025; Han, Kumar, and Tsvetkov 2023). Separately, remasking strategies have been proposed within the MDM framework (Wang et al. 2025a; Mounier and Idehpour 2025), allowing certain tokens to be remasked and resampled during generation to further improve flexibility and output quality.

3 Preliminary Experiments

In this section, we highlight two key challenges of widely adopted uncertainty-based sampling strategies when applied to advanced MDMs. Through two preliminary experiments, we demonstrate how these issues limit their effectiveness and hinder optimal generation quality.

3.1 Insufficient Global Trajectory Control

In autoregressive models (ARMs), the decoding order is strictly fixed: tokens are generated sequentially from left to right, with each token conditioned on all previously generated tokens. In contrast, MDMs permit tokens to be decoded in any arbitrary order, thereby enabling more flexible and adaptive generation processes.

However, our findings reveal that this is not the case. In practice, uncertainty-based sampling strategies consistently exhibit a distinctive “U-shaped” decoding trajectory: tokens at both sequence boundaries are decoded early, followed by a convergence toward the center (see Figure 1(a)). We attribute this pattern to the greedy nature of the sampler and the model’s tendency to assign high confidence to structurally predictable tokens, leading to their disproportionate prioritization. This hypothesis is further supported by our intervention experiment in Appendix A.3.

Building on this observation, we further investigate how decoding trajectories impact MDM performance on tasks with differing structural requirements. We systematically compare three strategies—greedy confidence-based sampling, semi-autoregressive (Semi-AR) sampling, and strictly left-to-right decoding—each inducing a distinct generation order (see Figure 1(a)–(c)). These strategies are evaluated on two representative benchmarks: GSM8K, which requires step-by-step logical reasoning, and 4×4 Sudoku, which emphasizes global constraint satisfaction. The results, shown in Figure 1(d), reveal a sharp contrast: on GSM8K, confidence-based sampling performs worst, achieving only 6.8% accu-

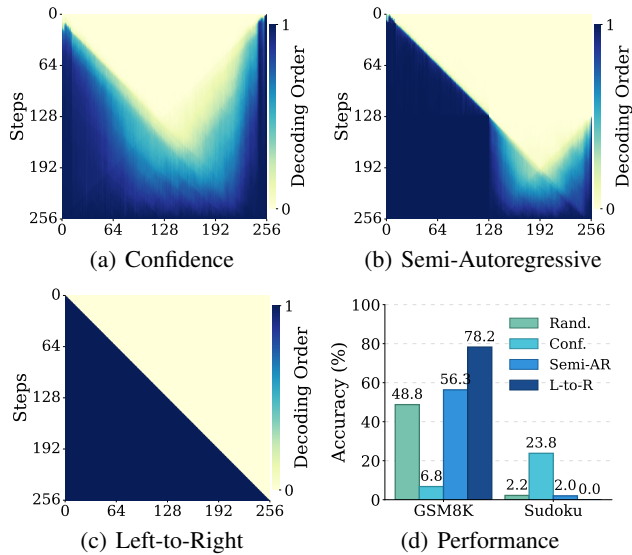


Figure 1: Visualization of average decoding trajectories on GSM8K for (a) confidence-based sampling, (b) confidence-based sampling with semi-autoregressive control, and (c) strictly left-to-right decoding. Each token position is assigned 1 from its unmasking step onward, and 0 otherwise. The averaged heatmap illustrates the typical decoding order for each position. Results for entropy-based and margin-based sampling strategies, as well as for other datasets exhibiting similar trends, are provided in Appendix A.2.

racy. In contrast, on Sudoku, it attains the highest accuracy at 23.8%, outperforming both Semi-AR and L-to-R decoding.

These results confirm that MDM performance remains highly sensitive to decoding order, as also noted in prior work (Kim et al. 2025). This sensitivity suggests that no single decoding strategy is universally optimal across tasks. Therefore, enabling explicit and flexible control over the generation trajectory—so that the model can adapt its decoding behavior to task-specific requirements—is essential for fully realizing the potential of MDMs in diverse application scenarios.

3.2 Trivial Token Bias

We further observe that uncertainty-based samplers tend to over-prioritize semantically trivial and high-frequency tokens—such as “`<EOS>`,” “`\n`,” “`.`,” “`the`,” “`is`,” and “`<SPACE>`”—during the early stages of decoding. These tokens commonly occur in the training corpus but contribute little to the semantic content of the generated sequence. This phenomenon arises primarily because such tokens often receive extreme confidence scores, making them “easy” targets for uncertainty-based sampling.

We empirically validate this phenomenon by analyzing the selection ratios and probabilities of trivial versus non-trivial tokens at the early decoding steps. As shown in Figure 2, trivial tokens overwhelmingly dominate the initial stages of generation: their selection ratios consistently exceed 80% during the first few steps, and their selection prob-

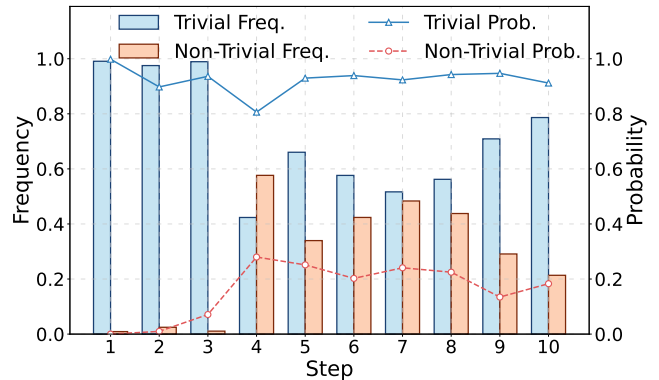


Figure 2: Statistics comparing trivial and non-trivial tokens during early decoding steps. Bars indicate the frequency of each token type at each step, while lines show the probability of selecting each type over time. See Appendix A.4 for the complete list of tokens defined as trivial, and Figure 13 for step-wise statistics of the most frequently selected tokens during early decoding.

abilities are substantially higher than those of non-trivial tokens. Although these tokens are easy to predict, their early selection provides little meaningful information to the context. As a result, the model wastes valuable decoding steps on low-information content, which is particularly detrimental for tasks such as mathematical and logical reasoning (see Table 4 in the Appendix A.8 for an illustrative example and the resulting generation failure). This weakens the contextual foundation for subsequent predictions and leads to poorly conditioned decoding trajectories.

4 Methodology

In this section, we first introduce the basic concepts and notations of Masked Diffusion Models (MDMs) (§4.1). We then present Position-Aware Confidence-Calibrated decoding strategy (PC-Sampler), a novel sampling strategy designed to address the aforementioned challenges (§4.2).

4.1 Background of MDMs

MDMs have recently emerged as a powerful framework for sequence generation, offering greater flexibility in decoding order compared to traditional autoregressive models. This flexible generation process is made possible by a training paradigm that optimizes the model to reconstruct masked tokens independently of any fixed generation order. Notably, recent work (Nie et al. 2025b) demonstrates that MDM training can be efficiently formulated as cross-entropy minimization over masked tokens. Formally, given a clean input sequence x_0 sampled from the training data, a time step t drawn uniformly from $[0, 1]$, and a corrupted sequence x_t constructed by independently masking each token in x_0 with probability t , the model is trained to recover the original tokens at the masked positions. The loss function is given by:

$$\mathcal{L}_{\text{MDM}} = -\mathbb{E}_{t, x_0, x_t} \left[\frac{1}{t} \sum_{i=1}^L \mathbf{1}[x_t^i = \mathbf{M}] \log p_{\theta}(x_0^i \mid x_t) \right], \quad (1)$$

where $\mathbf{1}[\cdot]$ denotes the indicator function, which returns 1 if the token is the masked token \mathbf{M} and 0 otherwise; p_θ represents the denoiser parameterized by θ .

At inference time, an MDM generates a target sequence from a fully masked input x_T of length L by iteratively unmasking tokens over T steps. At each step t , the model selects one or more positions from the set of currently masked positions \mathcal{M}_t and predicts the corresponding token values conditioned on the partially revealed sequence. This process is repeated until all tokens are unmasked, resulting in the complete generated sequence.

4.2 Position-Aware Confidence-Calibrated Decoding Strategy

Modern MDM decoding relies heavily on the choice of sampling strategy, as the order in which masked tokens are revealed has a significant impact on generation quality (Zheng et al. 2025; Nie et al. 2025b). A widely adopted decoding strategy in MDMs is uncertainty-based sampling, which selects the next token position to reveal based on the model’s internal uncertainty estimates. This approach aims to guide the generation process by progressively filling in the most certain tokens first.

Formally, at each decoding step t , let x_t denote the current partially generated sequence and \mathcal{M}_t the set of currently masked positions. The sampler \mathcal{S}_{unc} assigns a score s_t^i to each $i \in \mathcal{M}_t$ based on the model’s predicted distribution for that position:

$$s_t^i = \mathcal{F}(p_\theta(x^i | x_t)), \quad (2)$$

where $p_\theta(x^i | x_t)$ is the model’s predicted distribution over vocabulary tokens at position i , and \mathcal{F} is a token-level uncertainty function (e.g., confidence, entropy, or margin). The position with the highest (or lowest, depending on \mathcal{F}) score is then selected for unmasking:

$$i^* = \arg \max_{i \in \mathcal{M}_t} s_t^i. \quad (3)$$

Then, a token is sampled at the selected position from the learned mask predictor $p_\theta(\cdot)$:

$$x_t^{i^*} \sim p_\theta(x_t^{i^*} | x_t), \quad (4)$$

and used to update the sequence. The masked token at position i^* in x_t is replaced with the sampled value $x_t^{i^*}$, resulting in a less noisy version x_{t-1} . This decoding process is repeated iteratively until all tokens are unmasked, yielding the final output sequence.

However, our preliminary experiments indicate that existing uncertainty-based sampling strategies still face several limitations when applied to advanced MDMs. To overcome these issues, we propose a new decoding strategy that assigns a composite score to each candidate position $i \in \mathcal{M}_t$, unifying two complementary objectives: global trajectory planning and content-aware informativeness maximization. By integrating both aspects into a single, adaptable scoring function, our approach generalizes and subsumes previous strategies as special cases, while providing explicit control over both the generation trajectory and information flow.

Specifically, this composite score replaces the uncertainty score defined in Equation 2 at each decoding step:

$$s_t^i = w^i \cdot \mathcal{C}_t^i, \quad (5)$$

where w^i encodes the global decoding plan, enabling flexible control over the generation order, and \mathcal{C}_t^i quantifies the informativeness and reliability of unmasking position i , promoting the selection of semantically rich and under-represented tokens over trivial or frequent ones. These two terms are complementary and jointly enable both trajectory control and content-aware token selection.

Global Trajectory Control To regulate the global decoding trajectory, we introduce the position-aware weight w^i , which modulates the selection priority of each candidate token according to its position within the sequence. Specifically, we adopt an exponential decay function:

$$w^i = e^{-\lambda \cdot i}, \quad (6)$$

where $\lambda \geq 0$ is a decay coefficient that controls the strength of the positional penalty. This design allows us to globally control the decoding order by adjusting the value of λ : a larger λ encourages a decoding pattern closer to the left-to-right paradigm, while smaller values permit more flexible or free-form generation trajectories.

Content-Aware Confidence Calibration To discourage the over-selection of generic or high-frequency tokens and promote more informative choices, we draw inspiration from (Zhang et al. 2024) and calibrate the original confidence score with a frequency-based adjustment:

$$\mathcal{C}_t^i = -p_\theta(x^i | x_t) \cdot \log p_{\mathcal{D}'}(x^i), \quad (7)$$

where $p_\theta(x^i | x_t)$ is the model’s predicted probability for token x^i , and $p_{\mathcal{D}'}(x^i)$ represents the token frequency distribution estimated from a publicly available corpus \mathcal{D}' . To avoid outlier scores for rare tokens, we clip \mathcal{C}_t^i at a clipping threshold α (Zhang et al. 2024):

$$\mathcal{C}_t^i = \min(\mathcal{C}_t^i, \alpha), \quad (8)$$

At each decoding step, we compute the composite scores for all masked positions, select the highest-scoring position for unmasking, and sample its token value from the model, repeating this process until the sequence is fully decoded.

5 Experimental Methodology

This section introduces the evaluation datasets and tasks, implementation details, and baseline approaches.

5.1 Datasets and Tasks

We conduct experiments on seven datasets spanning four categories to comprehensively evaluate the effectiveness of our method: (1) **Mathematical Reasoning**: GSM8K (Cobbe et al. 2021), a benchmark of multi-step grade school math problems, and MATH500 (Lightman et al. 2024), a subset of competition-level problems from the MATH (Hendrycks et al. 2021) dataset. (2) **Code Generation**: HumanEval (Chen et al. 2021), a set of hand-crafted

Python programming tasks, and MBPP (Austin et al. 2021c), a crowd-sourced Python problem set. (3) **Scientific Reasoning**: GPQA (Rein et al. 2023), a challenging multiple-choice dataset requiring advanced physics knowledge. (4) **Planning**: 4×4 Sudoku (Nolte et al. 2024), a constraint-based reasoning task on a 4×4 grid, and Countdown with 3 numbers (Ye et al. 2025a), which is a combinatorial arithmetic game requiring basic operations to reach a target number.

5.2 Implementation Details

We evaluate the effectiveness of our method on three SOTA, open-source MDMs: LLaDA-8B-Instruct (Nie et al. 2025b), LLaDA-1.5-8B (Zhu et al. 2025), and Dream-7B (Ye et al. 2025b). For most datasets, we follow the generation length settings in Nie et al. (2025b). For MBPP, however, the maximum length is set to 128, as longer outputs are unnecessary. The number of denoising steps is set equal to the target sequence length. The position decay coefficient λ is set to 0 for Sudoku, which requires global planning. For all other tasks, λ is set to 0.25 to promote sequential reasoning, except for Countdown, where it is set to 0.5. The clipping threshold α is set to 10 for all tasks. Further experimental details are provided in Appendix A.5.

5.3 Baselines

We compare PC-Sampler against a comprehensive set of strong baselines, covering both autoregressive models and a diverse suite of decoding strategies in MDMs. Details of all baselines are provided in Appendix A.6.

Autoregressive Models To benchmark MDMs against conventional sequence generation models, we include three state-of-the-art ARMs of comparable scale: LLaMA-3.1-8B-Instruct (Dubey et al. 2024), Mistral-7B-Instruct (Jiang et al. 2023), and Qwen-2.5-7B-Instruct (Yang et al. 2024).

Decoding Strategies in MDMs We evaluate PC-Sampler against a range of representative decoding strategies in MDMs to ensure a clear and comprehensive comparison. In addition to standard and uncertainty-based approaches, we also include several recent methods designed to accelerate decoding while maintaining high generation quality.

- **Uniform Sampler** (Austin et al. 2021b): The vanilla sampler in MDMs, which randomly selects tokens to unmask.
- **Uncertainty-based Samplers**: Select tokens based on model uncertainty estimates. Specifically, we consider three widely used proxies: confidence (Chang et al. 2022), entropy (Ben-Hamu et al. 2025), and margin (Kim et al. 2025).
- **Semi-autoregressive Sampler**¹ (Nie et al. 2025b): This sampler partitions the sequence into blocks and generates them sequentially, thereby providing a single form of global trajectory control. Within each block, tokens are decoded based on confidence scores.

¹The official sampler used in LLaDA and LLaDA-1.5.

- **Efficient Samplers**: We further include two recently proposed efficient samplers that accelerate decoding while maintaining high generation quality: **Entropy-Bounded (EB) Sampler** (Ben-Hamu et al. 2025) and **Fast-dLLM** (Wu et al. 2025).

6 Evaluation Results

In this section, we first present the overall performance of PC-Sampler compared to the baselines, followed by ablation results, hyperparameter analysis, and the integration of PC-Sampler with efficient decoding strategies.

6.1 Main Results

Table 1 presents the performance of PC-Sampler and all baseline methods on seven representative benchmarks.

PC-Sampler consistently achieves the best performance across the majority of evaluated tasks. For both LLaDA and LLaDA-1.5 models, PC-Sampler leads to significant improvements over all other decoding strategies, with average accuracy gains of 5.3% and 7.6% for the two models, respectively. Notably, the performance boost is especially pronounced on challenging reasoning tasks such as GSM8K and MATH500. For instance, on LLaDA-1.5-Instruct, PC-Sampler achieves 82.2% on GSM8K and 49.9% on MBPP, outperforming the strongest baseline by more than 3% on average—both results representing the highest scores among all methods. Beyond reasoning, our approach also consistently improves performance on code generation and planning tasks, demonstrating broad applicability across diverse benchmarks.

Uncertainty-based and Semi-AR methods struggle to generalize across tasks. Uncertainty-based methods such as confidence, entropy, and margin perform well on Sudoku, but often exhibit instability and substantial accuracy drops on more challenging tasks. For example, entropy and margin samplers achieve average scores more than 40% lower than PC-Sampler on HumanEval and GSM8K. This performance drop is associated with the U-shaped decoding trajectory typical of these methods, which often leads to premature answer generation and insufficient reasoning (see Appendix A.2 for details). Similarly, semi-autoregressive approaches like Semi-AR and Fast-dLLM are competitive on certain reasoning tasks (e.g., GSM8K), but underperform on planning tasks such as Sudoku due to their fixed sequential generation order, which limits the model’s ability to capture complex dependencies. In contrast, PC-Sampler consistently excels across all tasks, benefiting from its flexible and globally-aware control over the generation trajectory. These results highlight the importance of flexible decoding strategies that can adapt globally to diverse task requirements.

PC-Sampler substantially narrows, and even surpasses, the performance gap with similarly sized ARMs. When equipped with PC-Sampler, both LLaDA and LLaDA-1.5 achieve average accuracies (42.3% and 44.7%) that are competitive with or superior to leading ARMs such as Qwen-2.5-7B-Instruct (44.2%). Notably, PC-Sampler-enhanced MDMs not only close the gap on typical reasoning and coding benchmarks but also deliver substantially

Methods & LLMs	HumanEval	MBPP	GSM8K	MATH500	GPQA	Countdown	Sudoku	Avg.↑
<i>Autoregressive LLMs</i>								
LLaMA-3.1-8B-Instruct	53.1	56.7	83.9	23.8	31.0	27.0	0.0	39.4
Mistral-7B-Instruct	43.9	37.0	49.4	7.2	28.1	22.7	0.0	26.9
Qwen-2.5-7B-Instruct	78.1	62.8	71.9	64.2	32.8	0.0	0.0	44.2
<i>LLaDA-Instruct-8B</i>								
Uniform	15.2	24.6	48.8	15.0	29.0	14.4	2.2	21.3
Confidence	8.5	34.0	6.8	3.4	27.9	34.0	23.8	19.8
Entropy	3.1	28.6	2.2	3.8	28.4	33.8	1.6	14.5
Margin	13.4	36.3	11.1	1.8	28.4	33.9	26.6	21.6
EB-Sampler	6.1	29.0	1.6	3.6	29.9	34.1	24.2	18.4
Semi-AR [†]	<u>39.0</u>	<u>45.2</u>	77.9	27.6	27.7	32.6	0.0	35.7
Fast-dLLM [†]	35.4	44.7	<u>78.2</u>	<u>28.4</u>	28.6	11.4	24.2	<u>37.0</u>
PC-Sampler	43.3	47.3	79.3	34.0	28.6	36.3	27.6	42.3
<i>LLaDA-1.5-8B</i>								
Uniform	17.7	23.0	52.7	20.0	28.1	15.8	3.4	23.0
Confidence	18.9	40.5	19.2	5.4	29.0	33.8	24.8	24.5
Entropy	17.1	36.1	12.1	5.0	38.8	<u>34.7</u>	0.2	19.1
Margin	21.3	42.2	27.9	6.4	28.6	31.8	33.6	27.4
EB-Sampler	17.1	35.6	12.3	4.8	28.6	34.6	1.6	19.2
Semi-AR [†]	<u>39.6</u>	<u>46.8</u>	80.7	<u>34.2</u>	26.1	32.4	0.0	<u>37.1</u>
Fast-dLLM [†]	37.2	46.1	<u>80.8</u>	31.2	27.9	32.9	0.4	36.7
PC-Sampler	46.3	49.9	82.2	37.4	28.8	35.0	<u>33.4</u>	44.7

Table 1: Experimental results on coding, mathematical reasoning, scientific reasoning, and logical reasoning tasks. We report pass@1 (%) for coding tasks and accuracy (%) for all other tasks. The best performance in each group is highlighted in **bold**, and the second-best is underlined. Following prior practices (Nie et al. 2025b; Zhao et al. 2025), we adopt a 4-shot setting for GSM8K and MATH500, a 5-shot setting for GPQA and Sudoku, a 0-shot setting for HumanEval and MBPP, and a 3-shot setting for Countdown. Methods marked with [†] denote samplers using the semi-autoregressive strategy, where the number of decoding blocks is set to 8 for all datasets. Results on Dream are provided in Table 2 in Appendix A.7.

higher accuracy on planning tasks like Countdown and Sudoku, domains where conventional ARMs often underperform. These results demonstrate that, with an effective decoding strategy, advanced MDM architectures are capable of matching or even surpassing the sequence generation performance of conventional ARMs of similar size. This paves the way for broader adoption of non-autoregressive generative models in practical applications.

6.2 Ablation Studies

We conduct ablation studies on LLaDA to evaluate the individual and combined effectiveness of our two key components: Global Trajectory Control and Content-Aware Confidence Calibration. The results are presented in Figure 3.

Effectiveness of Global Trajectory Control First, we assess the effectiveness of Global Trajectory Control by evaluating a variant that uses only this module (“w/ Traj. Ctrl.”) against the confidence-only baseline (“confidence”). As shown in Figure 3(a), introducing global trajectory control alone yields substantial performance gains. On the reasoning-intensive GSM8K task, accuracy increases dramatically from 6.75% to 64.37%. A similar improvement is observed on MBPP, where performance rises from 33.96% to 43.79%. These results underscore the importance of incorporating global trajectory constraints in the generation process, rather than relying solely on local decisions.

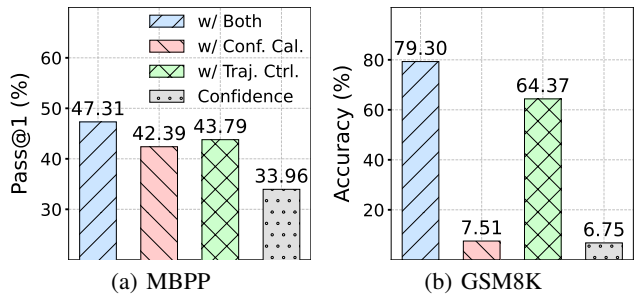


Figure 3: Ablation study results on the MBPP and GSM8K. “w/ Both” denotes our PC-Sampler, “w/ Conf. Cal.” denotes PC-Sampler without global trajectory control, “w/ Traj. Ctrl.” denotes PC-Sampler without content-aware confidence calibration.

Effectiveness of Content-Aware Confidence Calibration Next, we evaluate the impact of Content-Aware Confidence Calibration by comparing a variant that uses only this component (“w/ Conf. Cal.”) to the confidence-only baseline. The results show that confidence calibration independently leads to notable performance improvements, especially on MBPP, where performance increases from 33.96% to 42.39%. This demonstrates the effectiveness of content-

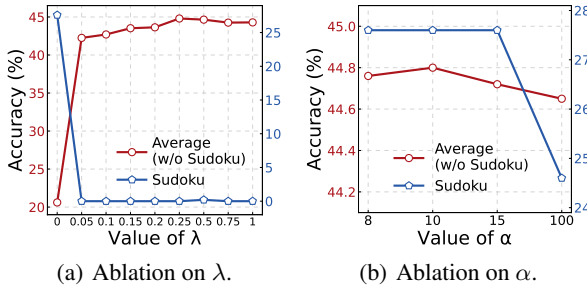


Figure 4: Ablation studies on the two key hyperparameters in our approach: (a) the positional decay coefficient λ and (b) the clipping threshold α . To analyze task-dependent effects, we split the evaluation into two groups: the blue line shows the average performance across all datasets except Sudoku, while the orange line shows the performance specifically on Sudoku.

aware calibration in refining token selection during generation by reducing the early output of uninformative tokens.

Complementary Effect of Both Components Finally, when both modules are combined (“w/ Both”), we observe the best overall performance, significantly surpassing either component alone. This demonstrates a clear and effective complementary effect, as the joint use of global trajectory control and content-aware calibration enables our method to fully realize its potential and achieve state-of-the-art results.

6.3 Hyperparameter Study

We conduct an ablation study to analyze the impact of two key hyperparameters in PC-Sampler: the positional decay coefficient λ and the clipping threshold α . Results are summarized in Figure 4.

Figure 4(a) shows that λ significantly influences performance in a task-dependent manner. For most tasks except Sudoku, a moderate value ($\lambda = 0.25$) achieves the best results by providing an appropriate positional bias. In contrast, larger values enforce a strictly left-to-right decoding order, which reduces flexibility and degrades accuracy. In contrast, tasks like Sudoku that require global constraint satisfaction benefit from smaller λ values. These findings demonstrate that the optimal λ setting varies with task structure: smaller values suit tasks demanding global planning, while larger values benefit step-by-step reasoning. This highlights that different tasks require different decoding trajectories. By enabling flexible tuning of λ according to the specific characteristics of each task, our approach demonstrates strong practicality and adaptability across diverse scenarios.

In Figure 4(b), we observe that model performance is relatively robust to the choice of α , with results remaining stable across all settings except the extreme case of $\alpha = 100$. Outside of this outlier, the performance exhibits minimal fluctuation. Based on these empirical findings, we recommend using a moderate value, specifically, $\alpha = 10$, as it consistently provides stable results across diverse tasks.

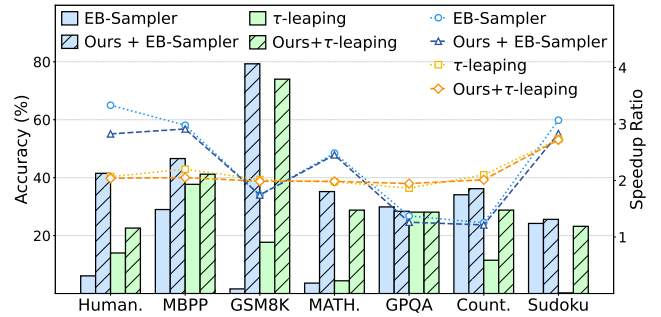


Figure 5: Performance and efficiency analysis of PC-Sampler integrated with efficient decoding strategies. Bar heights indicate accuracy, while lines (secondary y-axis) represent the speedup ratio relative to the vanilla MDM decoding strategy. For τ -leaping, τ is set to 2.

6.4 Integrating PC-Sampler with Efficient Decoding Strategies

In this subsection, we investigate the compatibility of PC-Sampler with efficient decoding frameworks, as generation efficiency plays a crucial role in the real-world applicability of MDMs (Israel, Broeck, and Grover 2025). Specifically, we integrate PC-Sampler as the token selection module into two representative approaches: τ -leaping (Chen et al. 2023), which decodes τ tokens per step, and EB-Sampler (Kim et al. 2025), an adaptive strategy that leverages error prediction to reveal multiple tokens while controlling error rates. The experimental setup follows our main protocol, evaluating both generation quality and decoding speed.

As shown in Figure 5, PC-Sampler can be seamlessly and effectively combined with both τ -leaping and EB-Sampler, consistently delivering higher accuracy than their respective baselines across nearly all evaluated benchmarks. The improvements are particularly notable on challenging reasoning tasks such as GSM8K and MATH, with average gains exceeding 10%. Importantly, the integration preserves most of the speedup benefits from multi-token decoding, achieving an average of $2 \times$ faster inference than vanilla decoding strategies, with only a minor reduction in efficiency compared to the fastest baseline configurations.

Overall, these findings highlight the remarkable flexibility and practical value of PC-Sampler, demonstrating that it can be effectively combined with efficient decoding strategies to achieve both high generation quality and accelerated inference. This substantially broadens and enhances the real-world applicability of MDMs.

7 Conclusion

In this work, we identify two fundamental limitations in existing decoding strategies for Masked Diffusion Models: a lack of global trajectory control and a strong bias toward trivial tokens during decoding. To address these challenges, we propose PC-Sampler, a position-aware confidence-calibrated decoding strategy that unifies global trajectory planning with content-aware informativeness maximization. Extensive experiments on a range of advanced MDMs and

diverse benchmarks demonstrate that PC-Sampler consistently outperforms existing methods, achieving substantial improvements in generation quality and narrowing the gap with state-of-the-art autoregressive models. Furthermore, we show that PC-Sampler is highly compatible with efficient decoding frameworks, enabling both high-quality and accelerated inference without additional training.

References

Arriola, M.; Gokaslan, A.; Chiu, J. T.; Yang, Z.; Qi, Z.; Han, J.; Sahoo, S. S.; and Kuleshov, V. 2025. Block Diffusion: Interpolating Between Autoregressive and Diffusion Language Models. In *The Thirteenth International Conference on Learning Representations, ICLR 2025, Singapore, April 24-28, 2025*.

Austin, J.; Johnson, D. D.; Ho, J.; Tarlow, D.; and van den Berg, R. 2021a. Structured Denoising Diffusion Models in Discrete State-Spaces. In Ranzato, M.; Beygelzimer, A.; Dauphin, Y.; Liang, P.; and Vaughan, J. W., eds., *Advances in Neural Information Processing Systems*, volume 34, 17981–17993. Curran Associates, Inc.

Austin, J.; Johnson, D. D.; Ho, J.; Tarlow, D.; and van den Berg, R. 2021b. Structured Denoising Diffusion Models in Discrete State-Spaces. In *Advances in Neural Information Processing Systems 34: Annual Conference on Neural Information Processing Systems 2021, NeurIPS 2021, December 6-14, 2021, virtual*, 17981–17993.

Austin, J.; Odena, A.; Nye, M. I.; Bosma, M.; Michalewski, H.; Dohan, D.; Jiang, E.; Cai, C. J.; Terry, M.; Le, Q. V.; and Sutton, C. 2021c. Program Synthesis with Large Language Models. *CoRR*.

Bai, J.; Bai, S.; Chu, Y.; Cui, Z.; Dang, K.; Deng, X.; Fan, Y.; Ge, W.; Han, Y.; and Huang, F. 2023. Qwen Technical Report. *CoRR*.

Ben-Hamu, H.; Gat, I.; Severo, D.; Nolte, N.; and Karrer, B. 2025. Accelerated Sampling from Masked Diffusion Models via Entropy Bounded Unmasking. *ArXiv preprint*.

Campbell, A.; Yim, J.; Barzilay, R.; Rainforth, T.; and Jaakkola, T. S. 2024. Generative Flows on Discrete State-Spaces: Enabling Multimodal Flows with Applications to Protein Co-Design. In *Forty-first International Conference on Machine Learning, ICML 2024, Vienna, Austria, July 21-27, 2024*.

Chang, H.; Zhang, H.; Jiang, L.; Liu, C.; and Freeman, W. T. 2022. MaskGIT: Masked Generative Image Transformer. In *IEEE/CVF Conference on Computer Vision and Pattern Recognition, CVPR 2022, New Orleans, LA, USA, June 18-24, 2022*, 11305–11315.

Chen, C.; Borgeaud, S.; Irving, G.; Lespiau, J.; Sifre, L.; and Jumper, J. 2023. Accelerating Large Language Model Decoding with Speculative Sampling. *CoRR*.

Chen, M.; Tworek, J.; Jun, H.; Yuan, Q.; de Oliveira Pinto, H. P.; Kaplan, J.; and Edwards, H. 2021. Evaluating Large Language Models Trained on Code. *CoRR*.

Christopher, J. K.; Bartoldson, B. R.; Ben-Nun, T.; Cardei, M.; Kailkhura, B.; and Fioretto, F. 2025. Speculative Diffusion Decoding: Accelerating Language Generation through Diffusion. In *Proceedings of the 2025 Conference of the Nations of the Americas Chapter of the Association for Computational Linguistics: Human Language Technologies, NAACL 2025 - Volume 1: Long Papers, Albuquerque, New Mexico, USA, April 29 - May 4, 2025*, 12042–12059.

Cobbe, K.; Kosaraju, V.; Bavarian, M.; Chen, M.; Jun, H.; Kaiser, L.; Plappert, M.; Tworek, J.; Hilton, J.; Nakano, R.; Hesse, C.; and Schulman, J. 2021. Training Verifiers to Solve Math Word Problems. *CoRR*.

DeepSeek-AI; Guo, D.; Yang, D.; Zhang, H.; Song, J.; Zhang, R.; Xu, R.; Zhu, Q.; and Ma, S. 2025. DeepSeek-R1: Incentivizing Reasoning Capability in LLMs via Reinforcement Learning. *CoRR*.

Dhariwal, P.; and Nichol, A. Q. 2021. Diffusion Models Beat GANs on Image Synthesis. In *Advances in Neural Information Processing Systems 34: Annual Conference on Neural Information Processing Systems 2021, NeurIPS 2021, December 6-14, 2021, virtual*, 8780–8794.

Dubey, A.; Jauhri, A.; Pandey, A.; Kadian, A.; Al-Dahle, A.; Letman, A.; and Mathur, A. 2024. The Llama 3 Herd of Models. *CoRR*.

Gong, S.; Agarwal, S.; Zhang, Y.; Ye, J.; Zheng, L.; Li, M.; An, C.; Zhao, P.; Bi, W.; Han, J.; Peng, H.; and Kong, L. 2025. Scaling Diffusion Language Models via Adaptation from Autoregressive Models. In *The Thirteenth International Conference on Learning Representations, ICLR 2025, Singapore, April 24-28, 2025*.

Gong, S.; Li, M.; Feng, J.; Wu, Z.; and Kong, L. 2023. DiffuSeq: Sequence to Sequence Text Generation with Diffusion Models. In *The Eleventh International Conference on Learning Representations, ICLR 2023, Kigali, Rwanda, May 1-5, 2023*.

Han, X.; Kumar, S.; and Tsvetkov, Y. 2023. SSD-LM: Semi-autoregressive Simplex-based Diffusion Language Model for Text Generation and Modular Control. In *Proceedings of the 61st Annual Meeting of the Association for Computational Linguistics (Volume 1: Long Papers), ACL 2023, Toronto, Canada, July 9-14, 2023*, 11575–11596.

He, Z.; Sun, T.; Tang, Q.; Wang, K.; Huang, X.; and Qiu, X. 2023. DiffusionBERT: Improving Generative Masked Language Models with Diffusion Models. In *Proceedings of the 61st Annual Meeting of the Association for Computational Linguistics (Volume 1: Long Papers), ACL 2023, Toronto, Canada, July 9-14, 2023*, 4521–4534.

Hendrycks, D.; Burns, C.; Kadavath, S.; Arora, A.; Basart, S.; Tang, E.; Song, D.; and Steinhardt, J. 2021. Measuring Mathematical Problem Solving With the MATH Dataset. In Vanschoren, J.; and Yeung, S., eds., *Proceedings of the Neural Information Processing Systems Track on Datasets and Benchmarks 1, NeurIPS Datasets and Benchmarks 2021, December 2021, virtual*.

Ho, J.; Jain, A.; and Abbeel, P. 2020. Denoising Diffusion Probabilistic Models. In *Advances in Neural Information Processing Systems 33: Annual Conference on Neural Information Processing Systems 2020, NeurIPS 2020, December 6-12, 2020, virtual*.

Huang, P.; Liu, Z.; Yan, Y.; Yi, X.; Chen, H.; Liu, Z.; Sun, M.; Xiao, T.; Yu, G.; and Xiong, C. 2025a. Pip-kag: Mitigating knowledge conflicts in knowledge-augmented generation via parametric pruning. *arXiv preprint arXiv:2502.15543*.

Huang, Z.; Chen, Z.; Wang, Z.; Li, T.; and Qi, G. 2025b. Reinforcing the Diffusion Chain of Lateral Thought with Diffusion Language Models. *CoRR*.

Israel, D.; Broeck, G. V. d.; and Grover, A. 2025. Accelerating Diffusion LLMs via Adaptive Parallel Decoding. *CoRR*.

Jiang, A. Q.; Sablayrolles, A.; Mensch, A.; Bamford, C.; Chaplot, D. S.; de Las Casas, D.; Bressand, F.; Lengyel, G.; Lample, G.; Saulnier, L.; Lavaud, L. R.; Lachaux, M.; Stock, P.; Scao, T. L.; Lavril, T.; Wang, T.; Lacroix, T.; and Sayed, W. E. 2023. Mistral 7B. *CoRR*.

Kim, J.; Shah, K.; Kontonis, V.; Kakade, S. M.; and Chen, S. 2025. Train for the Worst, Plan for the Best: Understanding Token Ordering in Masked Diffusions. *CoRR*.

Koh, H.; Jhang, M.; Kim, D.; Lee, S.; and Jung, K. 2024. PLM-Based Discrete Diffusion Language Models with Entropy-Adaptive Gibbs Sampling. *CoRR*.

Kong, Z.; Ping, W.; Huang, J.; Zhao, K.; and Catanzaro, B. 2021. DiffWave: A Versatile Diffusion Model for Audio Synthesis. In *9th International Conference on Learning Representations, ICLR 2021, Virtual Event, Austria, May 3-7, 2021*. OpenReview.net.

Li, X.; Mei, S.; Liu, Z.; Yan, Y.; Wang, S.; Yu, S.; Zeng, Z.; Chen, H.; Yu, G.; Liu, Z.; et al. 2024. Rag-ddr: Optimizing retrieval-augmented generation using differentiable data rewards. *arXiv preprint arXiv:2410.13509*.

Lightman, H.; Kosaraju, V.; Burda, Y.; Edwards, H.; Baker, B.; Lee, T.; Leike, J.; Schulman, J.; Sutskever, I.; and Cobbe, K. 2024. Let's Verify Step by Step. In *The Twelfth International Conference on Learning Representations, ICLR 2024, Vienna, Austria, May 7-11, 2024*.

Liu, S.; Nam, J.; Campbell, A.; Stärk, H.; Xu, Y.; Jaakkola, T. S.; and Gómez-Bombarelli, R. 2025. Think while You Generate: Discrete Diffusion with Planned Denoising. In *The Thirteenth International Conference on Learning Representations, ICLR 2025, Singapore, April 24-28, 2025*.

Lou, A.; Meng, C.; and Ermon, S. 2024. Discrete Diffusion Modeling by Estimating the Ratios of the Data Distribution. In *Forty-first International Conference on Machine Learning, ICML 2024, Vienna, Austria, July 21-27, 2024*.

Mounier, N.; and Idehpour, P. 2025. Review, Remask, Refine (R3): Process-Guided Block Diffusion for Text Generation. *ArXiv preprint*.

Nie, S.; Zhu, F.; Du, C.; Pang, T.; Liu, Q.; Zeng, G.; Lin, M.; and Li, C. 2025a. Scaling up Masked Diffusion Models on Text. In *The Thirteenth International Conference on Learning Representations, ICLR 2025, Singapore, April 24-28, 2025*.

Nie, S.; Zhu, F.; You, Z.; Zhang, X.; Ou, J.; Hu, J.; Zhou, J.; Lin, Y.; Wen, J.; and Li, C. 2025b. Large Language Diffusion Models.

Nolte, N.; Kitouni, O.; Williams, A.; Rabbat, M.; and Ibrahim, M. 2024. Transformers Can Navigate Mazes With Multi-Step Prediction. *CoRR*.

Park, Y.; Lai, C.; Hayakawa, S.; Takida, Y.; and Mitsufuji, Y. 2025. Jump Your Steps: Optimizing Sampling Schedule of Discrete Diffusion Models. In *The Thirteenth International Conference on Learning Representations, ICLR 2025, Singapore, April 24-28, 2025*.

Peng, Z.; Bezemek, Z.; Patel, S.; Rector-Brooks, J.; Yao, S.; Tong, A.; and Chatterjee, P. 2025. Path Planning for Masked Diffusion Model Sampling. *CoRR*.

Qin, T.; Alvarez-Melis, D.; Jelassi, S.; and Malach, E. 2025. To Backtrack or Not to Backtrack: When Sequential Search Limits Model Reasoning. *CoRR*.

Rein, D.; Hou, B. L.; Stickland, A. C.; Petty, J.; Pang, R. Y.; Dirani, J.; Michael, J.; and Bowman, S. R. 2023. GPQA: A Graduate-Level Google-Proof Q&A Benchmark. *CoRR*.

Wang, G.; Schiff, Y.; Sahoo, S. S.; and Kuleshov, V. 2025a. Remasking Discrete Diffusion Models with Inference-Time Scaling. *CoRR*.

Wang, Z.; Shi, J.; Heess, N.; Gretton, A.; and Titsias, M. K. 2025b. Learning-Order Autoregressive Models with Application to Molecular Graph Generation. *CoRR*.

Wei, J.; Wang, X.; Schuurmans, D.; Bosma, M.; Ichter, B.; Xia, F.; Chi, E. H.; Le, Q. V.; and Zhou, D. 2022. Chain-of-Thought Prompting Elicits Reasoning in Large Language Models. In *Advances in Neural Information Processing Systems 35: Annual Conference on Neural Information Processing Systems 2022, NeurIPS 2022, New Orleans, LA, USA, November 28 - December 9, 2022*.

Wu, C.; Zhang, H.; Xue, S.; Liu, Z.; Diao, S.; Zhu, L.; Luo, P.; Han, S.; and Xie, E. 2025. Fast-dllm: Training-free acceleration of diffusion llm by enabling kv cache and parallel decoding. *ArXiv preprint*.

Yang, A.; Yang, B.; Hui, B.; Zheng, B.; Yu, B.; Zhou, C.; Li, C.; and Li, C. 2024. Qwen2 Technical Report. *CoRR*, abs/2407.10671.

Ye, J.; Gao, J.; Gong, S.; Zheng, L.; Jiang, X.; Li, Z.; and Kong, L. 2025a. Beyond Autoregression: Discrete Diffusion for Complex Reasoning and Planning. In *The Thirteenth International Conference on Learning Representations, ICLR 2025, Singapore, April 24-28, 2025*.

Ye, J.; Xie, Z.; Zheng, L.; Gao, J.; Wu, Z.; Jiang, X.; Li, Z.; and Kong, L. 2025b. Dream 7B.

Zhang, W.; Zhang, R.; Guo, J.; de Rijke, M.; Fan, Y.; and Cheng, X. 2024. Pretraining Data Detection for Large Language Models: A Divergence-based Calibration Method. In *Proceedings of the 2024 Conference on Empirical Methods in Natural Language Processing, EMNLP 2024, Miami, FL, USA, November 12-16, 2024*, 5263–5274.

Zhao, S.; Gupta, D.; Zheng, Q.; and Grover, A. 2025. d1: Scaling Reasoning in Diffusion Large Language Models via Reinforcement Learning. *CoRR*.

Zheng, K.; Chen, Y.; Mao, H.; Liu, M.-Y.; Zhu, J.; and Zhang, Q. 2025. Masked Diffusion Models are Secretly Time-Agnostic Masked Models and Exploit Inaccurate Categorical Sampling.

Zhu, F.; Wang, R.; Nie, S.; Zhang, X.; Wu, C.; Hu, J.; Zhou, J.; Chen, J.; Lin, Y.; Wen, J.; and Li, C. 2025. LLaDA 1.5: Variance-Reduced Preference Optimization for Large Language Diffusion Models. *CoRR*.

A Appendix

A.1 License

The licenses for the datasets used in this study are as follows: HumanEval, MBPP, GSM8K, and MATH-500 are released under the MIT License; GPQA is released under the CC BY 4.0 License; and Countdown and Sudoku are released under the Apache License 2.0.

A.2 Visualization of Uncertainty-Based Sampling Trajectories Across Datasets

To systematically examine the generality of the “U-shaped” decoding trajectory, we visualize the generation orders induced by various uncertainty-based sampling strategies—including confidence-, entropy-, and margin-based samplers—across all major benchmark datasets. The resulting trajectory heatmaps for GSM8K (Figure 6), MBPP (Figure 7), HumanEval (Figure 8), GPQA (Figure 9), Countdown (Figure 10), and Sudoku (Figure 11) consistently exhibit the characteristic U-shaped pattern, regardless of the specific uncertainty metric or the nature of the task. These findings indicate that the early decoding of boundary tokens is a universal property of uncertainty-based approaches, rather than a peculiarity of any particular method or dataset. This persistent behavior underscores an inherent limitation of uncertainty-driven sampling and highlights the need for more adaptive decoding strategies.

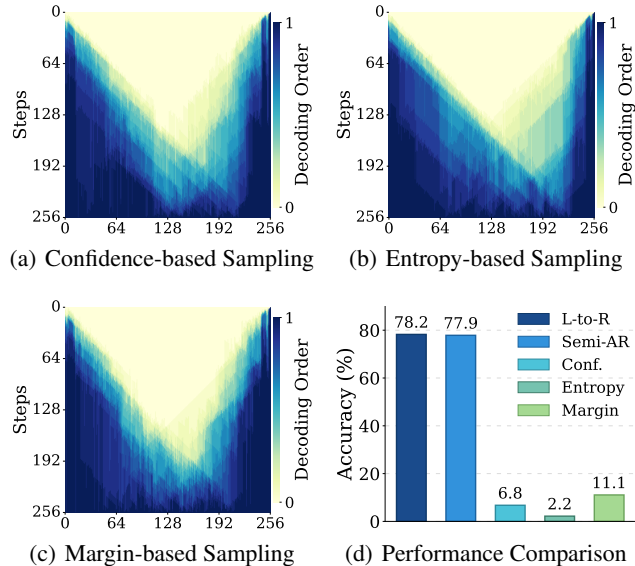


Figure 6: Visualization of decoding trajectories and performance for different uncertainty-based sampling methods on the GSM8K.

A.3 Intervention Analysis of the U-Shaped Trajectory

In this subsection, we establish the causal role of the sampler’s greedy nature and the model’s tendency to assign high confidence to structurally predictable tokens—often those

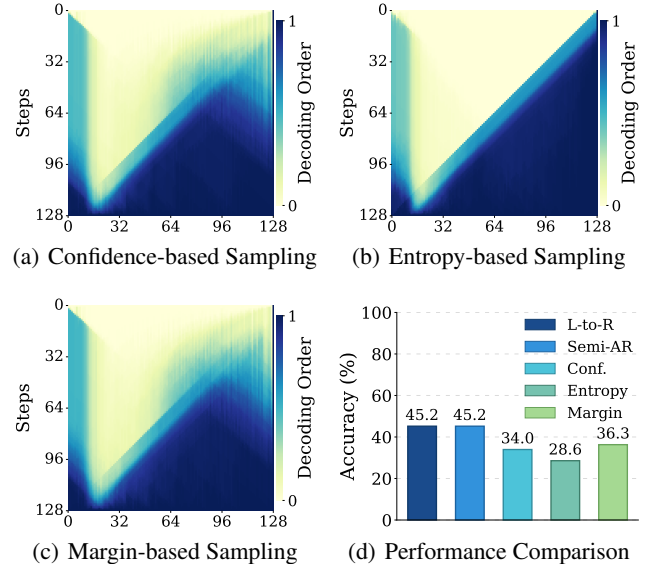


Figure 7: Visualization of decoding trajectories and performance for different uncertainty-based sampling methods on the MBPP.

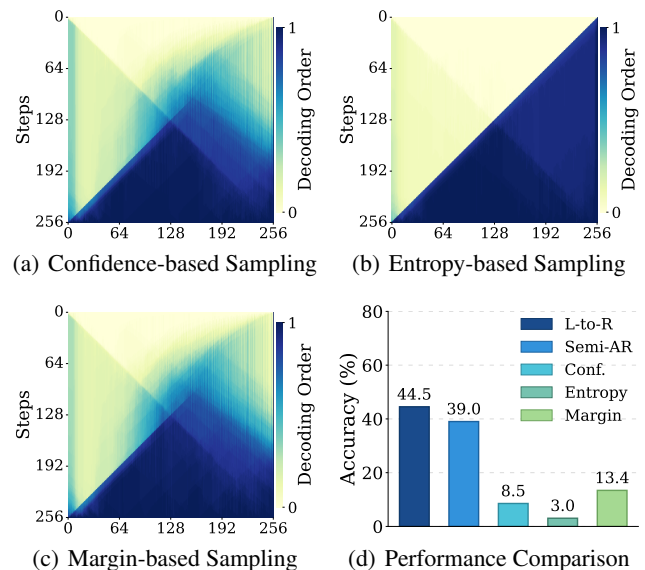


Figure 8: Visualization of decoding trajectories and performance for different uncertainty-based sampling methods on the HumanEval.

at the sequence boundaries—in producing the U-shaped decoding trajectory through intervention experiments.

Intervention Setup We conduct our intervention experiments on GSM8K using the LLaDA-8B-Instruct model. Specifically, the control group follows the standard uncertainty-based sampling strategy without any intervention to produce the decoding trajectory. In the experimental

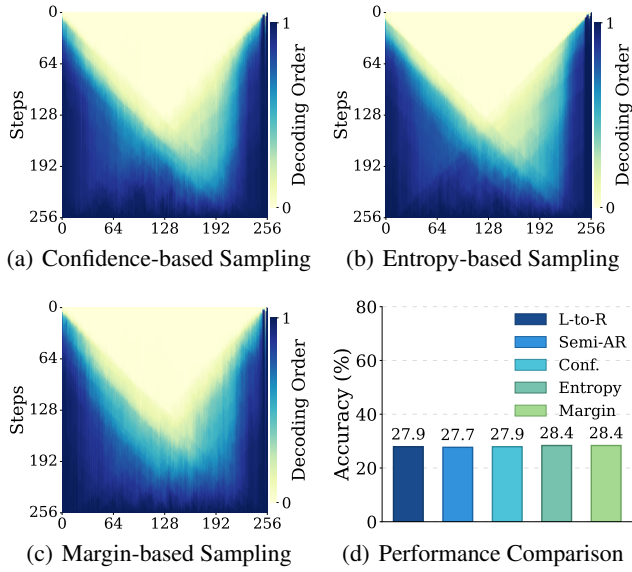


Figure 9: Visualization of decoding trajectories and performance for different uncertainty-based sampling methods on the GPQA.

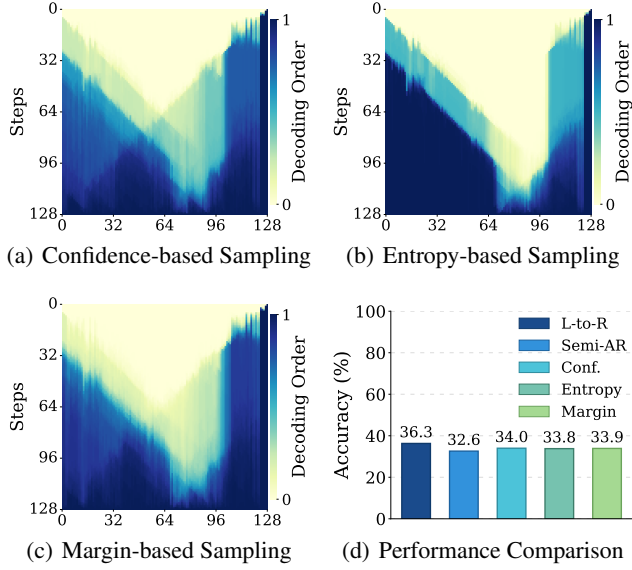


Figure 10: Visualization of decoding trajectories and performance for different uncertainty-based sampling methods on the Countdown.

group, we adopt a masking intervention strategy: during the initial decoding steps, boundary tokens are prohibited from being unmasked.

Results Figure 12 shows the decoding trajectories for both the control group and intervention groups. In the control group (“No Interference”, left), the U-shaped pattern is clearly observed: tokens at both sequence boundaries are decoded

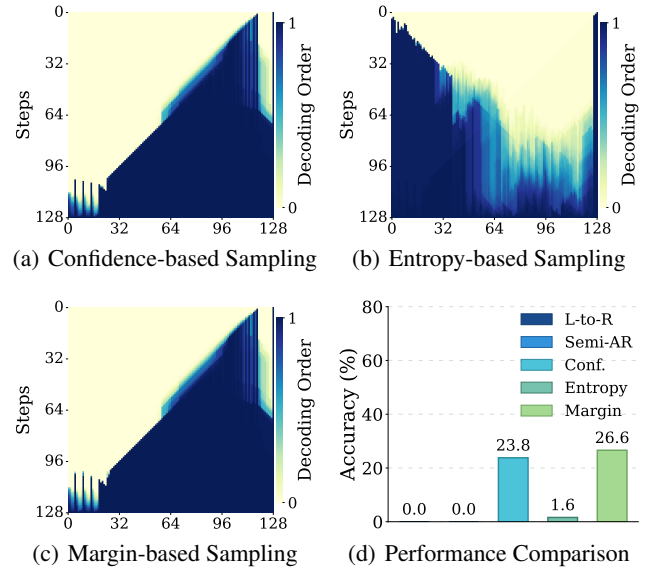


Figure 11: Visualization of decoding trajectories and performance for different uncertainty-based sampling methods on the Sudoku.

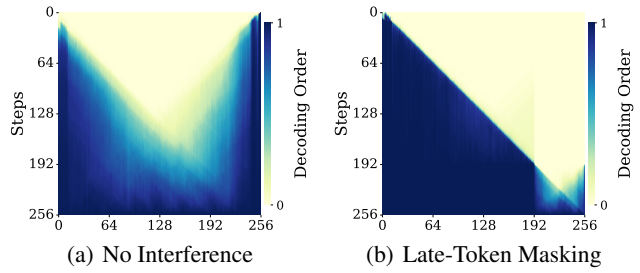


Figure 12: Intervention analysis isolating the cause of the U-shaped decoding trajectory. The control group (left), using standard confidence-based sampling, exhibits the pathological U-shaped pattern by prioritizing sequence boundaries. In contrast, the intervention group (right), where boundary tokens are masked during early decoding, reverts to a more natural left-to-right order.

early, with the generation trajectory converging toward the center in later steps. In contrast, under the masking intervention (“Late-Token Masking”, right), this U-shaped pattern is largely eliminated. The model is forced to prioritize the decoding of middle tokens, resulting in a decoding trajectory that proceeds more sequentially from the center outward. This marked shift in decoding order provides direct evidence that the U-shaped trajectory arises from the interplay between the sampler’s greedy selection and the model’s propensity to assign high confidence to structurally predictable tokens—particularly those at the sequence boundaries.

A.4 Detailed of Trivial Tokens

Definition of Trivial Tokens For our analysis, we define *trivial tokens* as a set of high-frequency tokens that frequently appear in the corpus but contribute limited semantic content. These include common structural symbols, punctuation marks, and filler words. The complete list of trivial tokens used in our study is provided below.

List of Trivial Tokens

```
<| endoftext |>  <| eot_id |>  <SPACE>
\n  .  ,  ?  !  :  ;  -  ( )  "  '  is
the  so  $  %
```

Early Decoding Bias Toward Trivial Tokens To quantitatively assess the prevalence of trivial tokens, we analyze their generation frequency during the initial stages of the diffusion process. Figure 13 shows the top five most frequent tokens generated in the first five decoding steps.

The results reveal a strong Trivial Token Bias: tokens such as `<| EOS |>` and `<| EOT |>`—which are expected to appear at the end of a sequence—are generated with very high frequency at the beginning. We also observe frequent early generation of prompt-related phrases such as “answer is”, as well as semantically uninformative tokens like “.”, `<| SPACE |>`, and other fillers, indicating a tendency to prematurely finalize outputs or insert meaningless content before sufficient reasoning has occurred.

These findings emphasize the necessity of our proposed calibration mechanism, which penalizes such high-frequency, low-information tokens and encourages more meaningful generation from the outset.

A.5 Additional Experiments Details

In this section, we provide a detailed description of our experimental setup and the implementation specifics of our proposed sampling strategy.

All experiments were conducted on NVIDIA A100 GPUs with 80GB of memory, using a default random seed of 42 to ensure reproducibility. During MDM inference, the temperature was set to 0.0 to guarantee deterministic and fully reproducible results. The calibrated confidence score in our PC-Sampler requires a background token frequency distribution. Following Zhang et al. (2024); Li et al. (2024), we constructed this distribution by aggregating several large-scale, publicly available text and code datasets. Specifically, we combined general-purpose text from BookCorpusOpen, mathematical reasoning problems from OpenR1-Math-220k, and all additional datasets used in our evaluation. Token frequencies were computed over this comprehensive corpus to provide a robust basis for calibration.

Evaluation Framework To ensure a fair and rigorous comparison, all baseline methods were evaluated using the same standardized evaluation procedures. For GSM8K and GPQA, we employed the widely used lm-evaluation-harness framework. For other tasks requiring specialized metrics or

formats, we adopted publicly available or officially recommended evaluation scripts, following (Nie et al. 2025a; Zhao et al. 2025; Huang et al. 2025a).

Prompting Strategies For GSM8K, GPQA, and MATH-500, we followed Nie et al. (2025a) and used the standard prompts provided in the lm-eval-harness framework. For HumanEval and MBPP, since Nie et al. (2025a) did not release the relevant prompt templates, we employed a custom prompt for all models as follows:

Prompt for Code Generation Tasks (HumanEval, MBPP)

Role: You are a professional Python coding assistant
Task: Complete the follow function implementation strictly and clearly without any additional comments or explanations.

{func}

Note: {func} is a placeholder for the function signature provided by the dataset.

For Sudoku, we used the prompt described in Zhao et al. (2025). For the Countdown task, we adopted the following prompt:

Prompt for Countdown Task

For the given numbers, find a sequence of arithmetic operations that results in the target number. Show your reasoning and conclude with “The answer is:”

A.6 Implementation Details of Baselines

This subsection details the implementation of the baseline methods evaluated in our experiments.

Uniform Sampling Strategy. This is the most basic sampling strategy for MDMs, where at each step a token is selected uniformly at random for decoding.

Confidence-Based Sampling Strategy. This is the most commonly used strategy, adopted by models such as LLaDA (Nie et al. 2025b). The score for a masked position i is given by the model’s predictive probability of its most likely candidate token v , conditioned on the current state x_t . The scoring function is defined as:

$$s_{\text{conf},t}^i = \max_{v \in \mathcal{V}} p_\theta(x_0^i = v \mid x_t), \quad (9)$$

where, \mathcal{V} denotes the vocabulary of the MDM. While straightforward, this approach offers substantial empirical advantages over uniform sampling.

Entropy-Based Sampling Strategy. This strategy evaluates the uncertainty of the entire predictive distribution by using entropy as a proxy (Ben-Hamu et al. 2025) at each position. A lower entropy indicates a more peaked and confident distribution. The score is given by the negative entropy of the distribution over the logits after applying the softmax function:

$$s_{\text{ent},t}^i = \sum_{v \in \mathcal{V}} p_\theta(x_0^i = v \mid x_t) \log p_\theta(x_0^i = v \mid x_t). \quad (10)$$

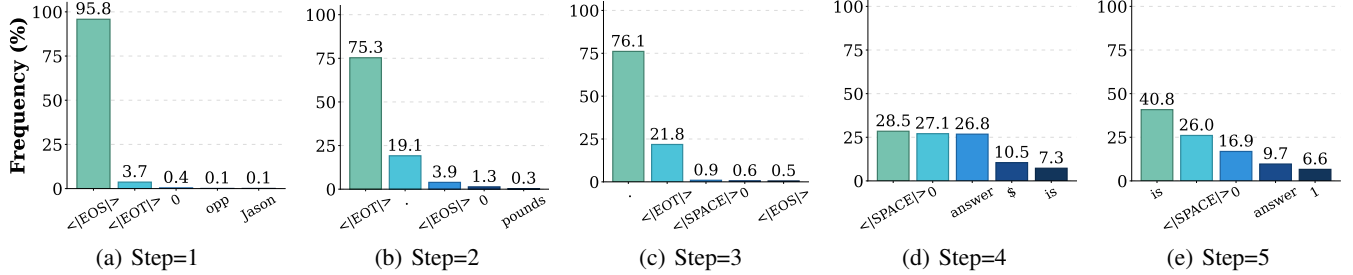


Figure 13: An analysis of the top-5 most frequent tokens across the initial five diffusion steps, corresponding to subfigures (a) through (e). This visualization clearly demonstrates that confidence-based decoding strategies have a strong tendency to generate trivial tokens, such as “<| EOS |>” and punctuation, during the early stages of the diffusion process.

Margin-Based Sampling Strategy. This alternative measures the model’s uncertainty by computing the probability margin between the two most confident candidate tokens at each position (Kim et al. 2025). A larger margin indicates a more decisive prediction. The score is defined as:

$$s_{\text{margin},t}^i = p_\theta(x_0^i = v_1 | x_t) - p_\theta(x_0^i = v_2 | x_t), \quad (11)$$

where v_1 and v_2 denote the two most likely tokens for position i according to the model’s predictive distribution $p_\theta(x_0^i | x_t)$.

EB-Sampler. The Entropy-Bounded Sampler (Ben-Hamu et al. 2025) accelerates generation by unmasking a variable number of tokens per step. The number of tokens is controlled by an error tolerance hyperparameter γ , which constrains the cumulative entropy to maintain generation quality. At each iteration, the masked tokens in \mathcal{M}_t are ranked by their entropy, and the largest subset is selected such that their joint dependency—approximated by the cumulative entropy—remains bounded as follows:

$$\sum_{i \in \mathcal{M}_t} H(p_\theta(\cdot | x_t)_i) - \max H(p_\theta(\cdot | x_t)_j) \leq \gamma, \quad (12)$$

where $H(\cdot)$ denotes the entropy of a token. This strategy enables more aggressive parallel decoding when predictions are confident, while falling back to more conservative, sequential decoding in cases of uncertainty.

Fast-dLLM. This sampler introduces a confidence-aware parallel decoding scheme to accelerate inference (Wu et al. 2025). Instead of unmasking a fixed number of tokens at each step, it unmasks all tokens whose confidence $p_\theta(x_0^i = v^i | x_t)$ exceeds a predefined threshold ϵ , where v^i denotes the most likely token at position i . This enables a dynamic number of tokens to be revealed in each iteration. Specifically, at each step, all positions i satisfying:

$$\max_{v \in \mathcal{V}} p_\theta(x_0^i = v | x_t) > \epsilon, \quad (13)$$

are unmasked in parallel.

Hyperparameter Settings for Baselines To ensure optimal performance for each baseline, we adopt the hyperparameter settings reported in prior work whenever available, or determine them through careful tuning otherwise. The detailed configurations are as follows:

- **EB-Sampler:** Following Israel, Broeck, and Grover (2025), we set the error tolerance parameter to $\gamma = 0.01$ for all datasets.
- **Fast-dLLM:** Following Wu et al. (2025), we set the confidence threshold to 0.9 for all datasets. The number of blocks in the semi-autoregressive sampler is fixed at 8 for HumanEval, MBPP, GSM8K, GPQA, and MATH500. For the Countdown and Sudoku datasets, a smaller block number of 4 is used, as a larger value of 8 leads to substantially lower performance.
- **Semi-AR:** We set the semi-autoregressive block count to a fixed value of 8 across all datasets.
- **Uncertainty-based Samplers:** These methods are evaluated without any semi-autoregressive decoding scheme in order to assess their performance under purely local, trajectory-unconstrained conditions.

A.7 Results on Dream

To further evaluate the generalization capability of our approach, we apply PC-Sampler to Dream-v0-Instruct-7B (Ye et al. 2025b), a SOTA Masked Diffusion Model developed independently of the LLaDA series (Nie et al. 2025a). As shown in Table 2, PC-Sampler consistently achieves the best performance across all evaluated tasks, with an average score of 40.1%. This represents a substantial improvement over the strongest uncertainty-based baseline, margin-based sampling, which reaches 27.8%. In particular, PC-Sampler achieves 57.9% on HumanEval and 76.4% on GSM8K, demonstrating strong performance in both code generation and mathematical reasoning tasks.

These results indicate that our method is not limited to a specific model family but instead addresses a fundamental limitation in MDMs. The observed tendency to prioritize boundary tokens early during decoding—especially due to supervised fine-tuning with EOS tokens—appears to be a systemic issue. By incorporating positional awareness into the sampling process, PC-Sampler mitigates this bias, allowing the model to allocate generation capacity more effectively and construct coherent, logically ordered outputs prior to boundary placement. The consistent gains observed across multiple tasks and model families underscore both the generality and practical utility of our approach.

Methods & LLMs	HumanEval	MBPP	GSM8K	MATH500	GPQA	Countdown	Sudoku	Avg.↑
<i>Autoregressive LLMs</i>								
LLaMA-3.1-8B-Instruct	53.1	56.7	83.9	23.8	31.0	27.0	0.0	39.4
Mistral-7B-Instruct	43.9	37.0	49.4	7.2	28.1	22.7	0.0	26.9
Qwen-2.5-7B-Instruct	78.1	62.8	71.9	64.2	32.8	0.0	0.0	44.2
<i>LLaDA-Instruct-8B</i>								
Uniform	15.2	24.6	48.8	15.0	29.0	14.4	2.2	21.3
Confidence	8.5	34.0	6.8	3.4	27.9	34.0	23.8	19.8
Entropy	3.1	28.6	2.2	3.8	28.4	33.8	1.6	14.5
Margin	13.4	36.3	11.1	1.8	28.4	33.9	26.6	21.6
EB-Sampler	6.1	29.0	1.6	3.6	29.9	34.1	24.2	18.4
Semi-AR [†]	<u>39.0</u>	<u>45.2</u>	77.9	27.6	27.7	32.6	0.0	35.7
Fast-dLLM [†]	35.4	44.7	<u>78.2</u>	<u>28.4</u>	28.6	11.4	24.2	<u>37.0</u>
PC-Sampler	43.3	47.3	79.3	34.0	28.6	36.3	27.6	42.3
<i>LLaDA-1.5-8B</i>								
Uniform	17.7	23.0	52.7	20.0	28.1	15.8	3.4	23.0
Confidence	18.9	40.5	19.2	5.4	29.0	33.8	24.8	24.5
Entropy	17.1	36.1	12.1	5.0	38.8	<u>34.7</u>	0.2	19.1
Margin	21.3	42.2	27.9	6.4	28.6	31.8	33.6	27.4
EB-Sampler	17.1	35.6	12.3	4.8	28.6	34.6	1.6	19.2
Semi-AR [†]	<u>39.6</u>	<u>46.8</u>	80.7	<u>34.2</u>	26.1	32.4	0.0	<u>37.1</u>
Fast-dLLM [†]	37.2	46.1	<u>80.8</u>	31.2	27.9	32.9	0.4	36.7
PC-Sampler	46.3	49.9	82.2	37.4	<u>28.8</u>	35.0	<u>33.4</u>	44.7
<i>Dream-v0-Instruct-7B</i>								
Uniform	17.7	31.9	31.5	17.0	32.8	4.1	0.2	19.3
Confidence	27.4	41.5	45.4	20.8	<u>35.3</u>	19.8	0.0	27.2
Entropy	26.2	42.4	36.8	17.0	33.5	<u>19.0</u>	0.0	25.0
Margin	<u>28.1</u>	41.7	<u>48.3</u>	<u>22.0</u>	35.7	<u>19.0</u>	0.0	<u>27.8</u>
EB-Sampler	<u>26.8</u>	<u>43.6</u>	37.5	17.4	33.3	18.6	0.0	25.3
Fast-dLLM	12.8	23.9	46.1	19.2	34.4	11.6	0.0	21.1
PC-Sampler	57.9	56.4	76.4	37.8	33.9	18.4	0.0	40.1

Table 2: Experimental results on coding, mathematical reasoning, scientific reasoning, and logical reasoning tasks. We report pass@1 (%) for coding tasks and accuracy (%) for all other tasks. The best performance in each group is highlighted in **bold**, and the second-best is underlined. For GSM8K and MATH500, we use a 4-shot setting; for GPQA and Sudoku, 5-shot; for HumanEval and MBPP, 0-shot; and for Countdown, 3-shot. All settings follow prior works (Nie et al. 2025b; Zhao et al. 2025) for fair comparison.

A.8 Case Study

In this subsection, we present two case studies in Table 3 and Table 4, drawn from the GSM8K (mathematical reasoning) and HumanEval (code generation) benchmarks, respectively. These cases compare the basic confidence-based sampling strategy with our proposed PC-Sampler approach.

As shown in the table, the main source of failure for the baseline confidence sampler is its inherent U-shaped bias and its tendency to favor trivial tokens. Our analysis reveals that this issue is largely attributable to the model’s propensity to generate structurally predictable tokens (i.e., trivial tokens as defined earlier), which often appear at the end of the sentence, too early in the decoding process. Combined with local attention bias, this causes the model to decode from right to left in certain segments, resulting in the characteristic U-shaped decoding trajectory. This restricts the subsequent generation path and frequently leads to incomplete or illogical outputs.

As illustrated in Table 3, the baseline is prone to generating trivial tokens prematurely. Due to local attention bias,

the model subsequently begins decoding leftward from the trivial token (i.e., $<|EOS|>$) position, resulting in the answer being produced before any reasoning steps are generated. This process ultimately leads to an incorrect and unjustified conclusion.

Similarly, for HumanEval (Table 4), the baseline’s early focus on trivial tokens often leads to premature sequence termination and incomplete code, resulting in significant wastage of the generation budget. In contrast, PC-Sampler mitigates this issue by incorporating position-aware weighting and content-aware confidence calibration, which introduce an inductive bias toward sequential reasoning. As a result, complete and correct code is generated before sequence termination.

These case studies demonstrate that explicit trajectory control is essential for complex reasoning and generation tasks. By mitigating both the U-shaped bias and the trivial token bias, PC-Sampler enables the model to produce outputs that are more coherent, accurate, and complete.

Case 1: Multi-Step Mathematical Reasoning (GSM8K)

Question	Judy teaches 5 dance classes, every day, on the weekdays and 8 classes on Saturday. If each class has 15 students and she charges \$15.00 per student, how much money does she make in 1 week?
Confidence (Baseline)	Judy teaches 5 dance classes every day on weekdays, so in one week, she teaches $5 * 5 = 25$ classes. Each class has 15 students, so in one week, she teaches $25 * 15 = 375$ students. She teaches 5 dance classes every day, so in one week, she teaches $5 * 15 = 75$ students. Additionally, she teaches 8 classes on Saturday. Each class has 15 students, so on Saturday, she teaches $8 * 15 = 120$ students. In total, in one week, she teaches $75 + 120 = 195$ students. Since she charges \$15.00 per student, she makes $195 * 15 = \$2975.00$ in 1 week. Final Answer: ##### 2975
Analysis	The baseline sampler locks in the incorrect final answer 2975 at an early stage . The subsequent reasoning steps are rendered ineffective as they are forced to align with a pre-determined, erroneous conclusion. This demonstrates a critical flaw where the model answers before it "thinks".
PC-Sampler (Ours)	Judy teaches 5 dance classes every day on weekdays, for a total of $5 \text{ days} * 5 \text{ classes/day} = 25 \text{ classes}$. On Saturday, she teaches 8 classes. So in one week, she teaches a total of $25 + 8 = 33$ classes. Each class has 15 students, so she teaches $33 * 15 = 495$ students. She charges \$15 per student, so she makes $495 * 15 = \$7425.00$ in one week. Final Answer: ##### 7425
Analysis	Our PC-Sampler follows a coherent, step-by-step reasoning process. It correctly calculates the total number of classes before determining the final income, leading to the correct answer. The generation order aligns with the logical flow of the problem.

Table 3: A case study on the GSM8K dataset illustrating how the generation order impacts multi-step mathematical reasoning. The baseline's premature commitment to an incorrect answer highlights a critical failure mode, whereas PC-Sampler's coherent process leads to the correct solution. The generation timing is color-coded as follows: Early Stage, Middle Stage, and Late Stage.

Case 2: Code Generation with Completeness (HumanEval)

Task	Implement the body of the Python function ‘has_close_elements’. The function should take a list of floats and a threshold, and return ‘True’ if any two distinct elements in the list are closer than the threshold, and ‘False’ otherwise.
Confidence (Baseline)	<pre>```python def has_close_elements(numbers: List[float], threshold: float) -> bool: for num in numbers: for other in numbers: if abs(num - other) < threshold: return True return False ```</pre> <p style="background-color: #ff9999; color: black; padding: 2px;">< endoftext > < endoftext > ... (many EOS tokens)</p>
	<i>Token Allocation: Code (~52 tokens) vs. Prematurely Generated EOS (~204 tokens)</i>
Analysis	The confidence-based sampler exhibits a catastrophic “U-shape” failure. It prematurely generates a large number of end-of-sequence (EOS) tokens in the early decoding stages. This drastically truncates the available space for code generation, forcing the model to output a rushed and incomplete solution. The resulting code is not only inefficient ($O(n^2)$) but also logically incorrect, as it fails to check that ‘num’ and ‘other’ are distinct elements, returning ‘True’ for any list if the threshold is positive.
PC-Sampler (Ours)	<pre>```python from typing import List def has_close_elements(numbers: List[float], threshold: float) -> bool: """ (A rigorous docstring with examples is generated here) """ for i in range(len(numbers)): for j in range(i + 1, len(numbers)): if abs(numbers[i] - numbers[j]) < threshold: return True return False ```</pre> <p style="background-color: #99ff99; color: black; padding: 2px;">< endoftext > < endoftext ></p>
	<i>Token Allocation: Code (~178 tokens) vs. Belatedly Generated EOS (~78 tokens)</i>
Analysis	By incorporating a positional bias, PC-Sampler generates the code in a natural, left-to-right order. It avoids the premature generation of EOS tokens, affording it the necessary space to first write out the full, descriptive docstring and then implement a correct and robust algorithm. The logic correctly compares only distinct pairs of elements, fulfilling all requirements of the task.

Table 4: Case study on the HumanEval dataset for code generation. The baseline method exhibits catastrophic failure due to the premature generation of trivial tokens, whereas PC-Sampler, through explicit trajectory control, produces robust and complete code. The generation timing is color-coded as follows: Early Stage, Middle Stage, and Late Stage.